

A regularised solution to the bridge weigh-in-motion equations

Eugene J. OBrien*

University College Dublin,

UCD School of Civil, Structural & Environmental Engineering, Newstead, Belfield, Dublin 4, Ireland

E-mail: eugene.obrien@ucd.ie

*Corresponding author

Cillian W. Rowley

Buro Happold,

17 Newman Street, London W1T1PD, UK

Fax: +44 870 787 4145

E-mail: cillian.rowley@burohappold.com

Arturo González

University College Dublin,

UCD School of Civil, Structural & Environmental Engineering, Newstead, Belfield, Dublin 4, Ireland

E-mail: arturo.gonzalez@ucd.ie

Mark F. Green

Department of Civil Engineering,

Queen's University at Kingston,

Ontario, Canada

Fax: +613-533-2128

E-mail: greenm@civil.queensu.ca

Abstract: The traditional approach to Bridge Weigh-in-Motion (WIM) developed by Moses, gives good accuracy for estimating gross vehicle weights but is less accurate for individual axle weights. In this paper, Tikhonov regularisation is applied to the original Moses' equations to reduce some of the inaccuracies inherent within the algorithm. The optimal regularisation parameter is calculated using the L-curve criterion. The new regularised solution is numerically tested using simulations of moving vehicles on a bridge. Results show that the regularised solution performs significantly better than the original approach of Moses and is insensitive to road surface roughness.

Keywords: bridge; WIM; weigh-in-motion; least squares minimisation; Tikhonov regularisation; L-curve; heavy vehicles; weights.

Reference to this paper should be made as follows: OBrien, E.J., Rowley, C.W., González, A. and Green, M.F. (2009) 'A regularised solution to the bridge weigh-in-motion equations', *Int. J. Heavy Vehicle Systems*, Vol. 16, No. 3, pp.310–327.

Biographical notes: Eugene J. OBrien obtained his PhD from Calgary in 1985. After five years in industry, he became a fulltime academic and has been Professor and Head of Civil Engineering in University College Dublin since 1998. He was a national delegate to COST 345, Chair of the Scientific Committee of the 4th Framework WAVE project and Vice-chair of COST 323 on WIM of Road

Vehicles. He has also participated in SAMARIS, ARCHES, ASSET European projects and currently leads the YEAR2010 project. He is president of the International Society for Weigh-in-Motion.

Cillian W. Rowley obtained his BE in Civil Engineering from University College Dublin in 2004. He obtained his PhD from University College Dublin in 2007. During his postgraduate studies, he published three conference papers, and one journal paper. He won the Lord Edward Fitzgerald Memorial fund prize for his outstanding achievements in moving force identification theory. Currently, he is working for Buro Happold in London.

Arturo González graduated in Civil Engineering at the University of Cantabria (Spain, 1995). He obtained MSc and PhD Degrees from Trinity College Dublin (Ireland, 1996 and 2001), specialising in bridge weigh-in-motion and vehicle-bridge interaction numerical and Finite Element models. Since 2001, he has been Piers Newman post-doctoral fellow and Lecturer in UCD School of Architecture, Landscape & Civil Engineering. He is author of 15 journal papers in the areas of bridge weigh-in-motion, structural dynamics, neural networks, traffic loading and bridge assessment. He is co-author of final reports for COST345 (2002), WAVE (1998) and ARCHES (2009) European framework projects.

Mark F. Green obtained his BSc from Queen's University (Kingston, Ontario) and PhD from the University of Cambridge in the UK. He was appointed to Queen's in 1993. He has published over 70 technical papers in bridge-vehicle dynamics and applications of fibre-reinforced polymers in concrete structures. He is Chair of the Canadian Society for Civil Engineering (CSCE) Technical Subcommittee on Advanced Composite Materials, and Co-chair of the American Concrete Institute (ACI) subcommittee 440-C. He has served as the Project Leader representative on the Board of Directors of ISIS Canada.

1 Introduction

Road authorities impose certain limits on vehicle size and weight to protect against severe pavement deterioration. The overloading of vehicles is not only a pavement and bridge design issue, but also affects fair competition in goods trading. Companies using overloaded vehicles can transport goods at less cost and therefore have an illegal competitive edge over their law-abiding rivals and other modes of transport such as rail. Another repercussion of overloading is traffic safety. Heavy goods vehicles are designed to operate within the boundaries of the law, which include speed limits as well as weight limits. By operating outside of these limits, the factor of safety employed in heavy goods vehicle design is reduced. Overloading may reduce the efficiency of braking, and the increased momentum of an overloaded vehicle would cause more damage if involved in a collision. It appears likely that a stricter enforcement of loading limits will lead to a decrease in road fatalities. Static weighing scales have been traditionally used to enforce overloading, but they cannot accommodate high volumes of truck traffic. Weigh-in-Motion (WIM) technology offers a solution to weigh trucks travelling at highway speeds automatically. WIM systems can pre-sort those trucks that are suspected of being overloaded to direct them to static scales, minimising unnecessary stops and delays for drivers.

A first division of WIM systems can be made by distinguishing On-Board WIM from Pavement- or Bridge-based WIM. The first group computes gross vehicle weight solely from measurements of force and acceleration taken through equipment in the vehicle (Chang et al., 2000). The second

group provides an independent measurement with respect to an On-Board WIM system, and it consists of measuring wheel effects in sensors mounted in or on the road pavement or on an existing bridge structure, and estimating the corresponding static loads with appropriate algorithms. Most WIM systems are based on weighing sensors that are embedded in the pavement or placed on top of the road surface and which measure wheel or axle pressure that is applied as the vehicle passes over them (Blab and Jacob, 2000; Caprez et al., 2000). As the effect of the applied force is recorded during a very short period of time, accuracy is limited by the dynamic nature of the vehicle motion. Additionally, these systems are subject to durability problems owing to traffic and the environment. An alternative approach to pavement WIM, which increases the length of the load-sensitive element and the durability of the system, is to use a bridge as a weighing scale (B-WIM); this approach is the subject of the research reported in this paper.

B-WIM is the process of finding truck axle weights from measured strains on a bridge as the truck crosses over it. Various algorithms, generally based on the static response of the bridge to a load, are used to infer vehicle axle weights from the measured strains. The original B-WIM equations were developed by Moses (1979) for application to composite beam and slab bridges. The algorithm is based on the principle of linear superposition, whereby the strains induced in the structure by the passage of a moving force are proportional to the product of the static axle weight and the corresponding influence ordinate. In the 1980s, Peters (1984) developed AXWAY in Australia. This B-WIM system is based on the same concept of influence line. A few years later, he derived a more effective system for weighing trucks using culverts, known as CULWAY (Peters, 1986). Both the American and Australian systems have been used for commercial applications on bridges and culverts. Bridge Weighing Systems Inc. developed one of the first commercial B-WIM systems in 1989 on the basis of Moses' algorithm (Snyder, 1992). In the 1990s, three new B-WIM systems were developed independently in Ireland, Slovenia and Japan (OBrien et al., 1999a; Žnidarič and Baumgärtner, 1998; Ojio et al., 2000). All of these B-WIM systems use algorithms based on static equations of equilibrium combined with measurements at one single longitudinal section. Many alternative approaches have been discussed in the literature (O'Connor and Chan, 1998; González et al., 2002; González, 2001) but Moses' algorithm and variations thereon still appear to be the basis for commercial B-WIM systems.

Low signal to noise ratios, inaccurate influence lines, and bridge and vehicle dynamics remain as sources of error for Moses' algorithm (OBrien et al., 1999b). Further, B-WIM systems generally tend to be more accurate for calculating gross weights than axle weights. This is because a long continuous strain record owing to the whole truck weight is available, but it is difficult to distinguish the contribution of each axle. McNulty and OBrien (2003) employed Moses' algorithm in major field tests and reported calculated gross vehicle weights being within 10% of the correct values with a confidence interval of 96.6%. The corresponding static axle weights were within 15% of the correct values with a confidence interval of 89.3%. The main reason for the relatively poor accuracy in axle weights is due to the ill-conditioned or ill-posed nature of the final system of equations used to solve the axle weights. This effect is particularly pronounced with closely spaced axles such as those in a tandem or tridem group. One solution to solve ill-posed systems of equations is to apply the mathematical tool of regularisation, whereby instead of attempting to solve the original system, a nearby better conditioned system is solved. This paper uses Tikhonov regularisation in combination with the L-curve for the selection of the optimal regularisation parameter to calculate the static axle

weights from the strain measurements. Results in static axle weights are considerably improved with respect to Moses' approach.

2 Moses' algorithm

For a static vehicle at a certain location on a girder bridge, the total longitudinal bending moment at a specific bridge section is defined as the sum of the individual moments in each girder. The bending moment, M_j^i , in each individual girder i at time step, j , is defined by equation (1).

$$M_j^i = E^i Z^i \varepsilon_j^i \quad (1)$$

where Z^i and E^i are the section modulus and the modulus of elasticity of the i^{th} girder, respectively, and ε_j^i is the measured strain at time step j at the soffit of the i^{th} girder. If the modulus of elasticity (E) and section modulus (Z) were the same for all girders, the total bending moment across the bridge section, M_j , at time step j is given by equation (2).

$$M_j = EZ \sum_{i=1}^g \varepsilon_j^i = EZ \varepsilon_j \quad (2)$$

where g is the number of girders and ε_j is the sum of the strain at all girders. For a truck crossing the bridge with n axles weighing $W_1 - W_n$, the theoretical static strain, $\hat{\varepsilon}_j$ at a particular time step j can be expressed by equation (3).

$$\hat{\varepsilon}_j = \frac{1}{EZ} [I_j^1 W_1 + I_j^2 W_2 + \dots + I_j^n W_n] \quad (3)$$

where I_j^i is the influence ordinate of total bending moment for the i^{th} axle at a particular point in time j . In practice, these influence ordinates can be obtained through an optimisation procedure using the bridge measurements corresponding to a calibration vehicle of known weights as proposed by OBrien et al. (2006). Equation (3) applies that for each time the strain is measured as dictated by the scan rate of the data acquisition equipment. Typical scan rates of 100–1000 Hz result in the massively over-determined system of equations given in equation (4).

$$\begin{Bmatrix} \hat{\varepsilon}_1 \\ \hat{\varepsilon}_2 \\ \hat{\varepsilon}_3 \\ \vdots \\ \vdots \\ \vdots \\ \hat{\varepsilon}_T \end{Bmatrix} = \frac{1}{EZ} \begin{bmatrix} I_1^1 & I_1^2 & \dots & I_1^n \\ I_2^1 & I_2^2 & \dots & I_2^n \\ I_3^1 & I_3^2 & \dots & I_3^n \\ \vdots & \vdots & \ddots & \vdots \\ \vdots & \vdots & \ddots & \vdots \\ \vdots & \vdots & \ddots & \vdots \\ I_T^1 & I_T^2 & \dots & I_T^n \end{bmatrix} \begin{Bmatrix} W_1 \\ W_2 \\ \vdots \\ W_n \end{Bmatrix} \quad (4)$$

where T is the number of readings, or in short form:

$$\{\hat{\varepsilon}\} = [A]\{W\} \quad (5)$$

where $\{\hat{\varepsilon}\}$ is the vector of theoretical static strain, $[A]$ is the matrix of influence ordinates for strain and $\{W\}$ is the vector of axle weights to be determined. This problem can be solved by minimising the sum of the squares of the differences between the theoretical and measured strains as given by equation (6).

$$\psi = \sum_{j=1}^T [\varepsilon_j - \hat{\varepsilon}_j]^2 \quad (6)$$

or, in matrix form

$$\psi = \{\varepsilon - [A]\{W\}\}^T \{\varepsilon - [A]\{W\}\}. \quad (7)$$

Expanding equation (7) yields an equation of the form

$$\psi = \{W\}^T [A]^T [A] \{W\} - 2\{W\}^T [A] \{\varepsilon\} + \{\varepsilon\}^T \{\varepsilon\}. \quad (8)$$

Minimising the objective function with respect to the vector of axle weights results in an equation of the form,

$$\{W\} = [F]^{-1} \{G\} \quad (9)$$

where

$$[F] = [A]^T [A] \quad (10)$$

$$\{G\} = [A]^T \{\varepsilon\}. \quad (11)$$

3 Regularised Moses' algorithm

3.1 Tikhonov regularisation

The method of Tikhonov regularisation (Tikhonov and Arsenin, 1977) minimises the linear combination given by equation (12):

$$W_\lambda = \min_W \{ \|[A]\{W\} - \{\varepsilon\}\|_2 + \lambda \|[A]\{W\}\|_2 \} \quad (12)$$

where λ is the regularisation parameter. The solution to the Tikhonov regularisation method is derived from the function $\hat{\psi}$ defined by equation (13).

$$\hat{\psi} = \{ \{\varepsilon\} - [A]\{W\} \}^T \{ \{\varepsilon\} - [A]\{W\} \} + \lambda \{W\}^T \{W\} \quad (13)$$

where λ is the non-negative regularisation parameter. Minimising the new objective function with respect to the vector of axle weights yields,

$$\frac{d\hat{\psi}}{dW_\lambda} = 2[A]^T ([A]\{W\}_\lambda - \{\varepsilon\}) + 2\lambda\{W\}_\lambda = 0. \quad (14)$$

The Tikhonov problem is then formulated as:

$$[[A]^T [A] + \lambda[I]]\{W\}_\lambda = [A]^T \{\varepsilon\} \quad (15)$$

where [I] is the identity matrix. The solution is now unique to each regularisation parameter λ and can be defined by:

$$\{W\}_\lambda = [[A]^T [A] + \lambda[I]]^{-1} [A]^T \{\varepsilon\}. \quad (16)$$

3.2 Selection of the regularisation parameter

The final stage in the regularisation of ill-posed problems is the choice of regularisation parameters. There are many methods in the current literature for calculating these parameters but most of them require some form of prior knowledge of the noise itself (Golub and van Loan, 1989). An efficient method is required for calculating the optimal regularisation parameter using only the available measurements. For inverse ill-posed problems of this nature, there are two methods in the current literature for obtaining the optimal regularisation parameter. These are Generalised Cross-Validation (Golub et al., 1979) and the L-curve method. The latter was first proposed by Lawson and Hanson (1974) and popularised by Hansen (1992, 1994, 1998) and is employed here. This method defines the residual norm of the error for each specific regularisation parameter as in equation (17).

$$E_{\text{norm}} = \sqrt{(\{\varepsilon\} - [A]\{W\}_\lambda)^T (\{\varepsilon\} - [A]\{W\}_\lambda)}. \quad (17)$$

It also defines the norm of the solution for each particular regularisation parameter as

shown in equation (18).

$$F_{norm} = \sqrt{\{W\}_{\lambda}^T \{W\}_{\lambda}} \quad (18)$$

The basic idea is to plot the discrete smoothing norm (F_{norm}) of the regularised solution vs. the residual norm (E_{norm}) on a log–log scale. Hansen (1998) has shown that in producing this, the plot will continuously depend on the smoothing parameter and that it will always have a corner where the optimal regularisation parameter is located.

With the addition of this side constraint in λ , the solution vector is no longer the solution of the linear system given in equations (8) and (9), but that of a new system, which seeks a fair balance between the residual norm and the solution norm. If $\lambda = 0$, then the problem is that of minimising the standard least squares; if λ is very large, the solution norm is small at the cost of a large residual norm. Hence, solving equation (12) involves a trade-off between the residual norm and the solution norm, this being determined by the single regularisation parameter λ . The procedure for the application of the regularised B-WIM (RB-WIM) approach is summarised in the flow diagram of Figure 1.

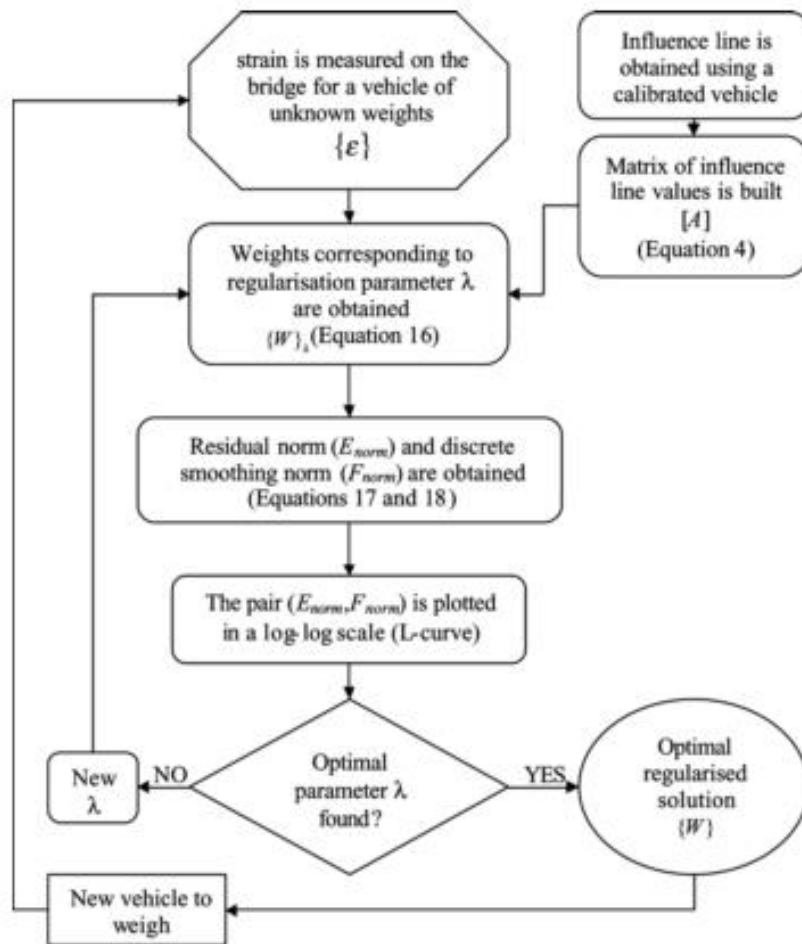


Figure 1 Flow diagram to obtain weights using RB-WIM

4 Testing

To examine the performance of the regularised solution of Moses' equations and compare it with that of the original equations, a strain signal at the mid-span of the bridge is required. The algorithm

is tested with three different vehicle models: a series of constant point loads representing vehicle axle weights, a series of sinusoidal loads, and an experimentally validated four-axle sprung vehicle. Vehicle inertial effects are ignored in the first two models, but the third model is composed of sprung and unsprung masses with their associated accelerations as a result of the interaction with the bridge and the pavement.

4.1 Moving constant loads

A 20 m simply supported beam model is used to demonstrate the application of regularisation theory to B-WIM. This bridge model has a cross-sectional area of 8 m² and second moment of area of 0.667 m⁴. The modulus of elasticity is 35 × 10⁹ N/m² and the density is 2400 kg/m³. The finite element method is used to simulate moving forces traversing the beam at constant velocity and constant axle spacing. The vehicle model consists of a series of constant loads representative of a typical three-axle truck (a front axle and a rear tandem with axle spacings of 4 and 1.5 m). Figure 2 shows the calculated mid-span strain at the bottom of the beam owing to the passage of the truck at a speed of 22 m/s. To simulate a measured signal, the theoretical strain is contaminated with Gaussian noise using equation (19).

$$\{\hat{\epsilon}\} = \{\hat{\epsilon}\} + \frac{r}{100} \hat{\epsilon}_{\max} \{N_{oise}\} \quad (19)$$

where $\{\hat{\epsilon}\}$ is the theoretical total strain, r is the percentage error, $\hat{\epsilon}_{\max}$ is the maximum strain induced in the simulation owing to the passage of the truck, and $\{Noise\}$ is a vector of random numbers with zero mean and a standard deviation of 1. Figure 3 shows the strain of Figure 2 contaminated with 2% Gaussian noise.

For the strain record of Figure 3, the regularisation parameter was varied between 1×10^{-90} and 600,000. Figure 4 shows the L-curve over this range of regularisation parameters, and Figure 5 shows the region where the optimal regularisation parameter lies. Figure 4 shows the distinctive shape of the L-curve while Figure 5 indicates that the optimal regularisation parameter lies between 90 and 500. Graphically, the point of maximum curvature is approximately 200.

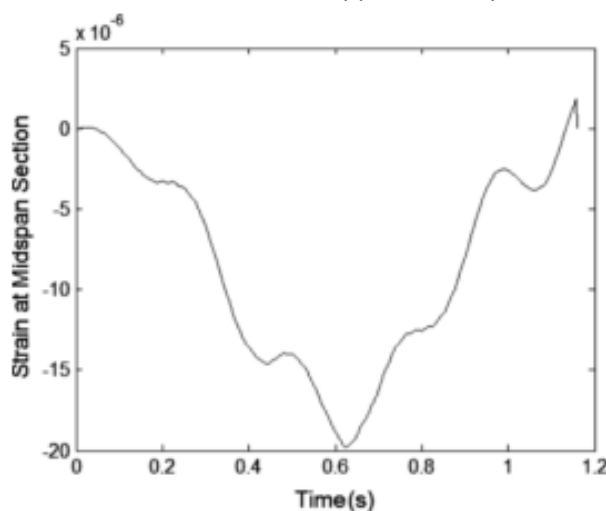


Figure 2 Theoretical total strain

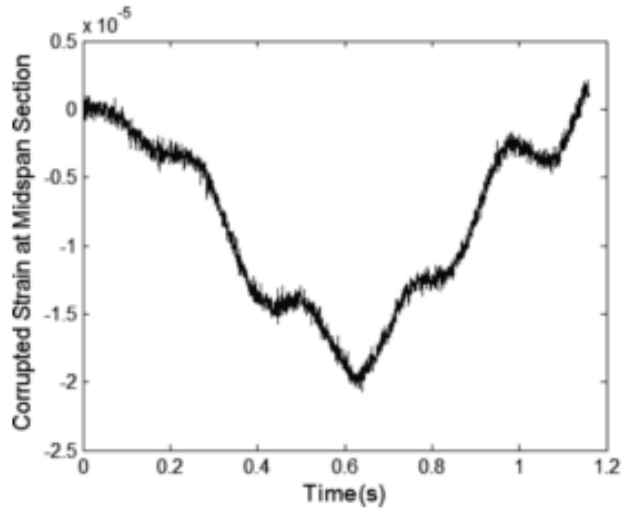


Figure 3 Simulated signal with 2% noise

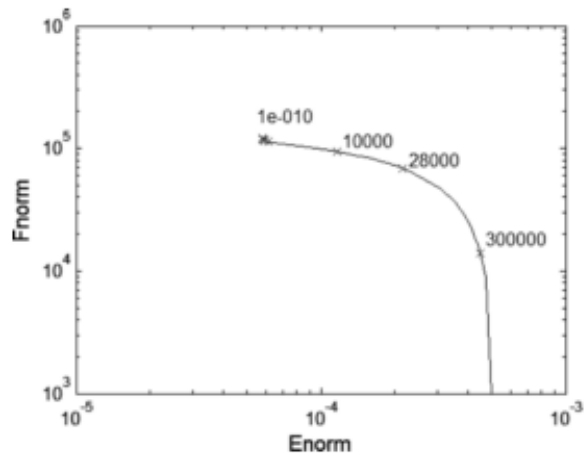


Figure 4 L-curve, full range of λ

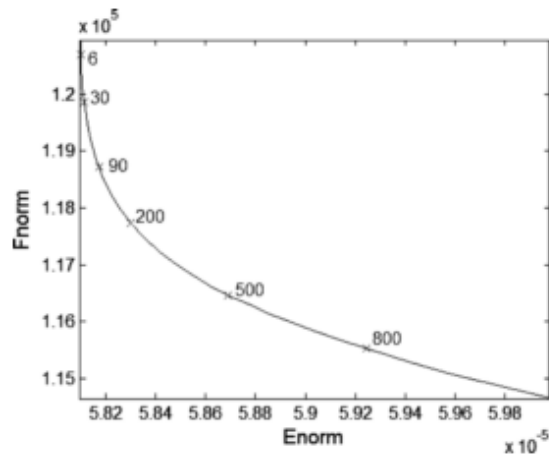


Figure 5 L-curve, adjacent to optimal λ

The axle weights corresponding to each regularisation parameter are given in Table 1. The exact weights are 60 kN, 80 kN and 60 kN for axles 1, 2 and 3 respectively. With $\lambda = 0$, the solution corresponds to Moses' equations. It can be seen that the 2% noise has resulted in significant

deviation (up to 16% error) from the static weights, particularly for the closely spaced axles 2 and 3. The optimally regularised solution (at about $\lambda = 200$) is considerably more accurate, approaching the exact axle weights with maximum errors of 2.5%.

Table 1 Regularised axle weights for a range of regularisation parameter values

λ	0	140	180	200	250	300	350	400
Axle 1 (kN)	56.9	59.7	59.8	60.1	60.4	60.5	60.7	60.7
Axle 2 (kN)	93.1	82.4	81.7	80.4	79.2	78.3	77.5	76.8
Axle 3 (kN)	52.1	60.1	60.6	61.5	62.3	62.9	63.3	63.7

Figure 6 illustrates the errors corresponding to the axle predictions in Table 1. The regularised solution represents a significant improvement in the accuracy of the inferred weight for all three axles.

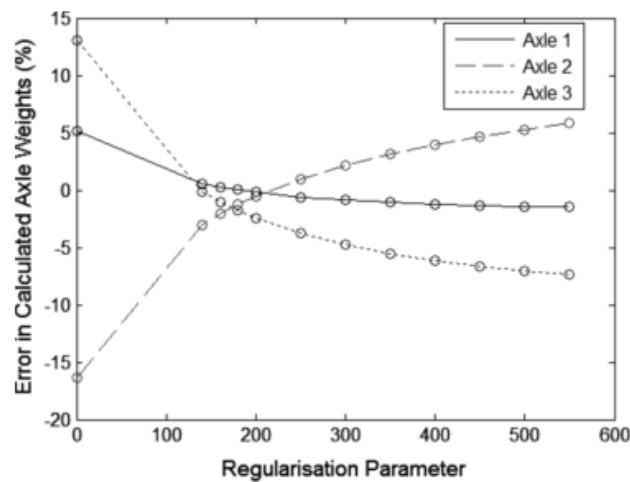


Figure 6 Error in predicted axle weights for a range of regularisation parameter λ values

4.2 Moving sinusoidal loads

To assess how the algorithm performs under axle dynamic oscillations, new simulations were carried out for the same vehicle configuration of Section 4.1, but where each axle force contained a time varying dynamic component defined by equation (20).

$$F_i(t) = W_i \left(1 + \frac{d}{100} \sin(5\pi t) \right) \quad (20)$$

where W_i is the static axle weight of the i th axle and d is a percentage representing the maximum dynamic increment. When d was varied from 1% to 5%, the regularised solution performed well. For higher levels of oscillation, the regularised solution failed to converge to the same extent. Nevertheless, the regularised solution gave better results than Moses' static algorithm in all cases. Figures 7 and 8 show the error in axle weights vs. a range of regularisation parameter values for 10% and 20% axle dynamic oscillations, respectively. Moses' algorithm had errors as high as 20% while the regularised solution had typical errors well below 10%.

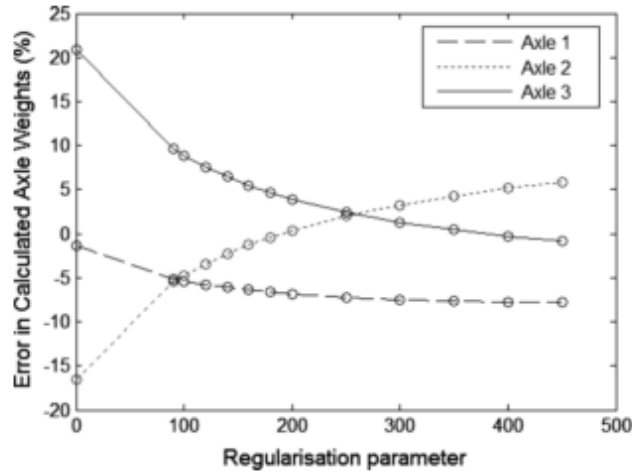


Figure 7 Error in axle weights for a range of regularisation parameter values and 10% axle dynamic oscillations

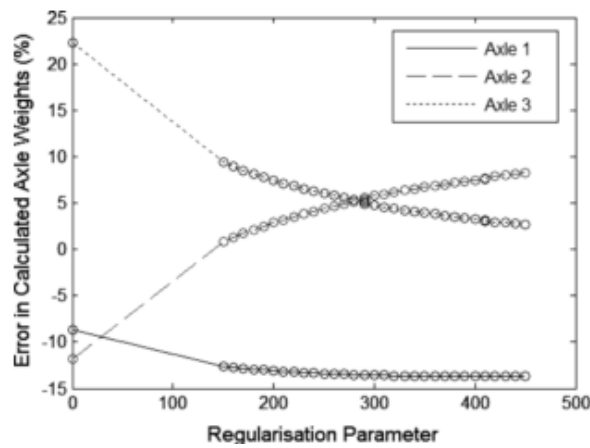


Figure 8 Error in axle weights for a range of regularisation parameter values and 20% axle dynamic oscillations

4.3 Moving sprung mass models

In this section, the bridge response is obtained through convolution of the vehicle loads with modal responses of the bridge. The convolution integral is solved by transformation to the frequency domain using the Fast Fourier Transform. The method is then extended by an iterative procedure to include dynamic interaction between the bridge and the mathematical model of the vehicle. Green and Cebon (1994) have illustrated the effectiveness of this calculation method, the convergence of the iterative procedure, and have reported good agreement with experimental data.

The bridge is modelled as a simply supported beam 30 m long, with a first natural frequency of 3.33 Hz and 1% damping. Strain output is calculated at mid-span of every 0.01 s (100 Hz). The B-WIM algorithm is calibrated, i.e., the influence line is found, with a two-axle fully laden linear sprung vehicle (four degrees of freedom). Then, the system is tested with the four-axle vehicle (11 degrees of freedom) of Figure 9 with two different suspension systems representing air and steel leaf. The test vehicle models employed here were developed by Green et al. (1995). In Figure 9, elements A, B and C represent non-linear suspension elements, linear springs, and a linear spring/damper

combination, respectively. For the vehicle with air suspension, models of air springs with parallel viscous dampers replace the steel-spring elements on the drive axle and the two trailer axles. The suspension on the steer axle is the same for both vehicle models. Two surface profiles, three different speeds (55, 70 and 85 km/h), and two different loading conditions are chosen for the simulations.

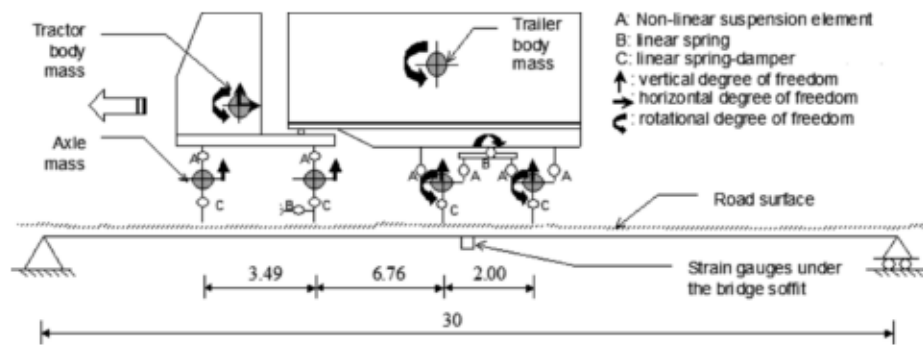


Figure 9 Scheme of vehicle and bridge models

4.4 Calibration

The shape of the theoretical influence line is known from beam theory and the static algorithm only requires a calibration factor to adjust the magnitude of the strains to the theoretical model. If the exact influence line for bending moment is used, the calibration factor is the product of the modulus of elasticity and the section modulus (equation (2)). In the case of an experimental record, there are several approaches that can be used to obtain the real shape of the influence line (OBrien et al., 2006). For this analysis, the calibration factor is obtained by dividing the real static gross vehicle weight by the predicted weight of the calibration truck. A linear sprung two-axle vehicle with 4 m axle spacing, 32.42 kN static weight in the front axle and 59.94 kN in the rear axle is used for calibration. The strain record generated by the two-axle vehicle is contaminated with 3% noise according to equation (19). The calibration factor changes very slightly with speed and an average value of 2.10×10^{10} is adopted.

4.5 Testing with four-axle truck on smooth road surface

Figure 10 shows the simulated strain owing to the passage of two fully laden four-axle vehicles at 70 km/h, differentiated by the suspension type only, before being corrupted with noise. As expected, the steel suspension causes higher dynamic oscillations in the strain signal than the air-suspension vehicle.

The % error in the estimation of the static axle weight by Moses' original algorithm and the proposed regularised algorithm is given in Figures 11 and 12, respectively. The results found by regularisation are generally much more accurate than found using the original B-WIM algorithm. The improvement is quite significant for axles within a group (3rd and 4th axles) owing to the inability of the original B-WIM algorithm to effectively separate weights of closely spaced axles. Table 2 summarises the results by both algorithms for the 12 sample runs (2 suspension types, 2 loading conditions and 3 speeds).

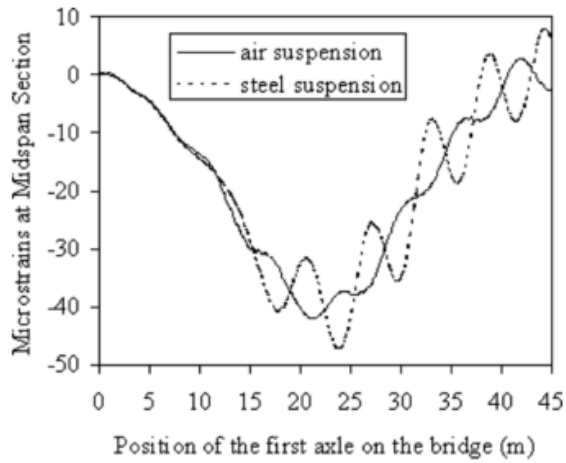


Figure 10 Theoretical total strain due to fully laden vehicle travelling at 70 km/h (smooth profile)

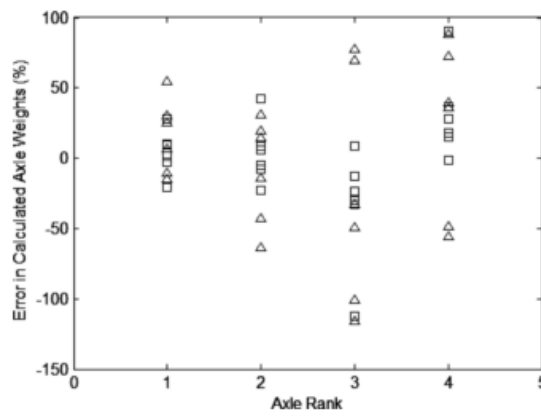


Figure 11 Error vs. axle rank for 4-axle truck by B-WIM (smooth profile) (□ air-sprung vehicle, Δ steel-sprung vehicle)

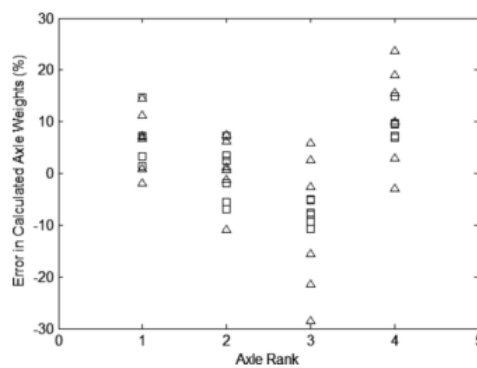


Figure 12 Error vs. axle rank for 4-axle truck by RB-WIM (smooth profile) (□ air-sprung vehicle, Δ steel-sprung vehicle)

Table 2 Relative error statistics by B- and RB-WIM algorithms on smooth profile

Criterion	Total number of runs	B-WIM			RB-WIM		
		Mean (%)	Standard deviation (%)	Maximum error (%)	Mean (%)	Standard deviation (%)	Maximum error (%)
Single axle	24	20.8	16.9	63.5	5.5	4.2	14.7
Axle within axle group	24	49.8	33.6	116.3	10.6	7.0	28.6
Gross weight	12	1.0	0.6	2.1	1.9	1.0	3.7

4.6 Testing with four-axle vehicle on rough road surface

On a rough profile, the maximum dynamic response takes place at 70 km/h for the steel-sprung vehicle and it is about three times that obtained on a smooth profile. The maximum dynamic response takes place at 85 km/h for the air-sprung vehicle. The air-suspended vehicle causes significantly lower dynamic bridge response than the steel-spring suspended vehicle and it is less sensitive to a change in speed. These high dynamics suggest the occurrence of frequency matching between the steel-sprung vehicle and the bridge. Consequently, Bridge WIM will tend to be less accurate in the cases of steel-spring suspensions, rough road profiles, and for this bridge, for vehicle speeds near 70 km/h.

Figures 13 and 14 show the % error in the estimation of static axle weights by both algorithms for all the runs of the four-axle vehicle on a rough profile. The error in the prediction of static axle weights increased considerably for the B-WIM algorithm (in many cases by over a few 100%). Although the errors by the RB-WIM algorithm have slightly increased overall, they are obviously less sensitive to the dynamic increment in the bridge response than B-WIM. The relative error statistics for both algorithms are presented in Table 3. Axle loads can also be calculated for more than one vehicle driving simultaneously on the bridge, once the vehicle position is known at each point in time. Nevertheless, a decrease in accuracy may be expected owing to the higher number of unknowns.

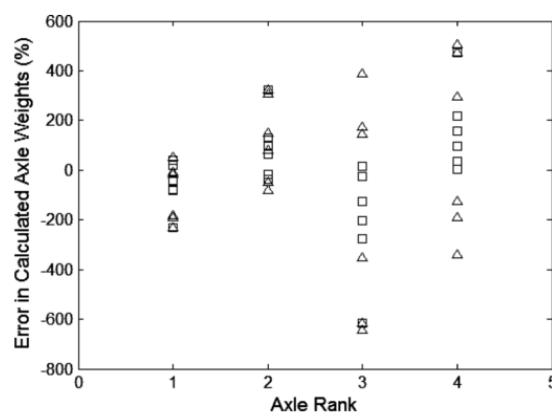


Figure 13 Error vs. axle rank for 4-axle truck by B-WIM (rough profile) (□ air-sprung vehicle, △ steel-sprung vehicle)

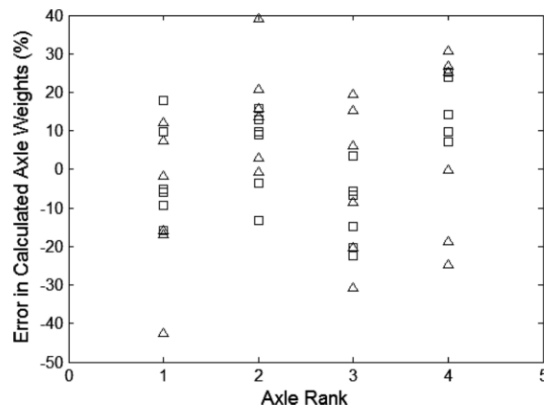


Figure 14 Error vs. axle rank for 4-axle truck by RB-WIM (rough profile) (□ air-sprung vehicle, Δ steel-sprung vehicle)

Table 3 Relative error statistics by B- and RB-WIM algorithms on rough profile

Criterion	Total number of runs	B-WIM			RB-WIM		
		Mean (%)	Standard deviation (%)	Maximum error (%)	Mean (%)	Standard deviation (%)	Maximum error (%)
Single axle	24	117.9	100.8	321.9	13.1	10.5	42.5
Axle within axle group	24	265.7	208.0	646.0	17.3	8.8	30.8
Gross weight	12	3.4	3.8	12.2	2.5	2.1	8.2

5 Conclusions

Information on the weights and configurations of heavy vehicles can be uninterruptedly collected using pavement- or bridge-based WIM systems. Then, WIM data can be used to predict future traffic volumes and weights for the planning of new constructions, the management of maintenance activities, the identification/reduction of overloading problems and the evaluation of the performance of pavements and bridges.

Compared with pavement-based WIM systems, B-WIM is increasing in popularity owing to its relatively low cost of installation, portability, minimal or null disruption to traffic, ease of maintenance and difficulty to be detected by a driver. Moses' algorithm remains as the basis for the calculation of vehicle weights in commercial B-WIM systems. One of its main advantages is its relatively good accuracy, in particular for gross vehicle weights, and the ease of its implementation compared with other theoretical developments requiring complex dynamic models and abundant instrumentation. This paper has presented an improvement in accuracy over Moses' original algorithm without increasing the needs for the B-WIM installation and calibration. This new B-WIM algorithm employs the method of Tikhonov regularisation in conjunction with Moses' equations. The method is theoretically tested using dynamic simulations of a series of moving forces on a bridge; it has been shown that, for low vehicular dynamics, the new algorithm significantly improves the errors in predicted axle weights inferred from Moses' algorithm. However, as the vehicle dynamics increase, the convergence of the regularised solution is not as acute. In any case, the regularised solution performs better than the original B-WIM algorithm.

Acknowledgements

Professor Eugene J. OBrien, Dr. Cillian W. Rowley and Dr. Arturo González express their gratitude for the financial support received from the 6th European Framework Project ARCHES (Assessment and Rehabilitation of Central European Highway Structures) towards this investigation. Dr. Mark F. Green thanks the Natural Sciences and Engineering Research Council (NSERC) of Canada for financial support of this project, Haiyin Xie for conducting the bridge–vehicle simulations, and David Cebon and David Cole for use of their vehicle simulation package.

References

- Blab, R. and Jacob, B. (2000) 'Test of a multiple sensor and four portable WIM systems', *International Journal of Heavy Vehicle Systems*, Vol. 7, Nos. 2–3, pp. 111–135.
- Caprez, M., Doupal, E., Jacob, B., OConnor, A.J. and OBrien, E.J. (2000) 'Vehicle based Weigh-in-Motion system', *International Journal of Heavy Vehicle Systems*, Vol. 7, Nos. 2–3, pp. 169–190.
- Chang, W., Sverdlova, N., Sonmez, U. and Streit, D. (2000) 'Vehicle based weigh-in-motion system', *International Journal of Heavy Vehicle Systems*, Vol. 7, Nos. 2–3, pp. 205–218.
- Golub, G.H. and van Loan, C.F. (1989) *Matrix Computations*, The John Hopkins University Press, Baltimore, Maryland, USA.
- Golub, G.H., Heath, M. and Wahba, G. (1979) 'Generalized cross-validation as a method for choosing a good ridge parameter', *Technometrics*, Vol. 21, No. 2, May, pp. 215–223.
- González, A., Green, M.F., OBrien, E.J. and Xie, H. (2002) 'Theoretical testing of a multiple-sensor bridge weigh-in-motion algorithm', *Proceedings of the Seventh International Symposium on Heavy Vehicle Weights and Dimensions (ISHVWD)*, Delft, The Netherlands, 16–20 June, pp.109–130.
- González, A. (2001) *Development of Accurate Methods of Weighing Trucks in Motion*, PhD Thesis, Trinity College Dublin, Ireland.
- Green, M. and Cebon, D. (1994) 'Dynamic response of highway bridges to heavy vehicle loads: theory and experimental validation', *Journal of Sound and Vibration*, Vol. 170, No. 1, February, pp. 51–78.
- Green, M., Cebon, D. and Cole, D.J. (1995) 'Effects of vehicle suspension design on dynamics of highway bridges', *Journal of Structural Engineering, ASCE*, Vol. 121, No. 2, February, pp. 272–282.
- Hansen, P.C. (1992) 'Analysis of discrete ill-posed problems by means of the L-curve', *SIAM Review*, Vol. 34, No. 4, pp.561–580.
- Hansen, P.C. (1994) 'Regularization tools: a matlab package for analysis and solution of discrete ill-posed problems', *Numerical Algorithms* 6, pp. 1–35.
- Hansen, P.C. (1998) Rank-deficient and Discrete Ill-posed Problems, Numerical Aspects of Linear Inversion, *Society for Industrial and Applied Mathematics (SIAM)*, Philadelphia, USA.
- Lawson, C.L. and Hanson, R.J. (1974) *Solving Least Squares Problems*, Prentice-Hall, Englewood Cliffs, New Jersey, USA.
- McNulty, P. and OBrien, E.J. (2003) 'Testing of bridge weigh-in-motion system in sub-arctic climate', *Journal of Testing and Evaluation*, Vol. 31, No. 6, pp. 1–10.

- Moses, F. (1979) 'Weigh-in-motion system using instrumented bridges', *Transportation Engineering Journal of ASCE*, Proceedings of the American Society of Civil Engineers, Vol. 105, No. TE3, May, pp. 233–249.
- O'Connor, C. and Chan, T.H.T. (1988) 'Wheel loads from bridge strains: laboratory studies', *Journal of Structural Engineering*, ASCE, Vol. 114, No. 8, August, pp. 1724–1740.
- OBrien, E.J., Dempsey, A., Žnidarič, A. and Baumgartner, W. (1999b) 'High-accuracy Bridge-WIM systems and future applications', in Jacob, B. (Ed.): *Proceedings of the Final Symposium of the Project Wave*, Hermes Science Publications, Paris, France, pp. 45–54.
- OBrien, E.J., Quilligan, M.J. and Karoumi, R. (2006) 'Calculating an influence line from direct measurements', *Bridge Engineering*, Proceedings of the Institution of Civil Engineers, 159(BE1), March, pp. 31–34.
- OBrien, E.J., Žnidarič, A. and Dempsey, A.T. (1999a) 'Comparison of two independently developed bridge weigh-in-motion systems', *Heavy Vehicle Systems, Int. J. Vehicle Design*, Vol. 6, Nos. 1–4, pp. 147–161.
- Ojio, T., Yamada, K. and Shinkai, H. (2000) 'BWIM systems using truss bridges', *Bridge Management Four*, in Ryall, M.J., Parker, G.A.R. and Harding, J.E. (Eds.), Thomas Telford, University of Surrey, UK, pp.378–386.
- Peters, R.J. (1984) 'AXWAY – a system to obtain vehicle axle weights', *Proceedings 12th ARRB Conference*, Hobart, Australia, Vol. 12, No. 1, pp.17–29.
- Peters, R.J. (1986) 'An unmanned and undetectable highway speed vehicle weighing system', *Proceedings 13th ARRB Conference*, Adelaide, Australia, Vol. 13, No. 6, pp.70–83.
- Snyder, R.E. (1992) Field Trials of Low-Cost Bridge WIM, in Publication FHWA-SA-92-014, Washington DC.
- Tikhonov, A.N. and Arsenin, V.Y. (1977) *Solutions of Ill-Posed Problems*, John Wiley & Sons, New York.
- Žnidarič, A. and Baumgärtner, W. (1998) 'Bridge weigh-in-motion systems – an overview', in OBrien, E.J. and Jacob, B. (Eds.): *Pre-proceedings of the 2nd European Conference on Weigh-In-Motion*, Lisbon, Portugal, pp.139–152.